AIAA JOURNAL
Vol. 45, No. 10, October 2007

Quasi-One-Dimensional Unsteady-Flow Procedure for Real Fluids

Roger L. Davis*
University of California, Davis, Davis, California 95616
and
Bryan T. Campbell†
Aerojet, Sacramento, California 95813-6000

DOI: 10.2514/1.25849

The numerical solution techniques, including explicit, point-implicit, and fully implicit schemes, used in a new quasi-one-dimensional procedure for the transient solution of real-fluid flows in system lines and volumes are presented. The procedure is coupled with a real-fluid properties database so that both compressible and incompressible fluids may be considered using the same code. The procedure was implemented in Matlab/Simulink and Fortran95 to allow for application on a wide variety of computer platforms. The computational efficiency of the various numerical methods is discussed to aid in selection of specific applications. Results for the transient flows of gaseous nitrogen and water in a simple pipe network are presented to demonstrate the capability of the current techniques and the unsteady-flow physics that can occur in system lines.

Nomenclature

A	=	cross-sectional flow area
A_p	=	perimeter
a_r	=	relative acceleration between inertial and absolute frames of reference (including gravity)
CFL	=	Courant–Friedrichs–Lewy number
c	=	speed of sound
E	=	total energy, $\rho(e + u^2/2)$
e	=	fluid internal energy
F	=	flux of mass, momentum, and energy
H	=	static fluid enthalpy
i	=	cell index
K	=	minor loss coefficient, $2\Delta p/(\rho u^2)$
k	=	temporal order of accuracy for Simulink `ode15s` solution methodology
m, n	=	index variables
p	=	static pressure
$\dot{q}$	=	heat flux input
S	=	source vector
t	=	time
U	=	fluid state vector
u	=	absolute velocity
u_r	=	relative velocity
V	=	fluid cell volume
x	=	distance along the solution domain
z	=	potential height above sea level
ρ	=	fluid density
τ_w	=	shear force (friction)

Presented as Paper 3911 at the 36th Fluid Dynamics Conference, San Francisco, CA, 5–8 June 2006; received 14 June 2006; revision received 11 May 2007; accepted for publication 29 May 2007.

*Professor, Mechanical and Aeronautical Engineering. Associate Fellow AIAA.

†Engineering Specialist, Systems Engineering, Department 5271, P.O. Box 13222. Member AIAA.

I. Introduction

THE simulation of unsteady flows of nonidealized fluids in system lines and volumes is of interest for a wide variety of applications and industries, including air-conditioning systems, water/steam/oil piping networks, refinery systems, gas-turbine secondary flowpath and cooling networks, and liquid rocket engine propellant lines. Several approaches for simulating the dynamic behavior of such fluid-transmission lines have been reported. The lumped-analysis approach treats a flow passage as a series of fluid control volumes that conserve mass and energy linked by flow resistance elements that compute the flow between the volumes [1]. Although this approach does conserve momentum in a quasi-steady sense at the flow resistances, the unsteady momentum term in the governing equations is omitted. Although so-called *continuity* waves can be captured using this approach, neglecting these terms leads to an inability to capture the true *dynamic* waves required for simulating phenomena such as water hammer and pressure surge [2]. Another approach uses the method of characteristics [3], which can be applied to hyperbolic partial differential equations. The governing equations for fluid flow are compatible with this method and it has been used for simulation of fluid-transmission lines [4]. Although the unsteady momentum terms are retained using this method, other problems, particularly at the boundaries of components, make it difficult to apply to a modular system-level simulation tool. Modal methods have also been used when solution in the frequency domain is possible [5]. This technique represents the pressure and velocity distributions in the flow domain as a sum of an infinite series of mode shapes, similar to a Fourier series solution. Although this method does present an elegant and efficient method for simulating idealized flows (e.g., incompressible, inviscid, laminar, etc.), the addition of turbulent flow, real-fluid properties, heat transfer, and phase change complicate the application of the method and reduce its attractiveness.

Because unsteady phenomena such as wave dynamics play an important role in the operation and testing of systems that contain fluid lines, a method that captures these transient effects is required. The development of a quasi-one-dimensional (1-D), unsteady, two-phase flow solver with heat transfer and real-fluid properties using standard finite-difference/control-volume solution methods is the subject of the present effort. Such a solver is geared toward modeling the dynamic behavior of fluid-filled lines and passages (i.e., the solution domain is much larger in one spatial dimension than in the others) accounting for the effects of a changing cross-sectional area. In addition, the solver must be suitable for use as a module in larger

system-level transient simulations of hydraulic and pneumatic systems, and so the solution method must be computationally efficient. The following sections describe the modeling approach, numerical methodologies, and test cases that were used during the development of this model. Results are then shown for transient pipe flow of both nitrogen and water as a demonstration of the numerical capability and fluid physics that can be captured with the current procedure.

II. Approach

The model developed here represents fluid lines and flow passages in which the length of the domain is much larger than the domain hydraulic diameter, and so a quasi-1-D flow (i.e., 1-D flow with area change) assumption is valid. For these types of components, flow separations and nonaxial velocities are minimal, hence the quasi-1-D assumption is valid. The solver is targeted to the commercial Simulink dynamic simulation software package from The MathWorks for integration into a larger suite of modules developed for simulating various systems. Simulink was selected because it offers a wide range of capabilities, over a dozen robust differential equation solvers, extensive documentation and technical support, a modern graphically based modeling paradigm, an existing user community across many disciplines, and commercially funded code development and maintenance. A Fortran95 code using more traditional solution methods is also being developed in parallel, to provide verification test cases for the Simulink module.

The equation system is being developed to account for varying flow area, friction, minor losses (e.g., bends and fittings), real-fluid and two-phase flow effects, gravity and acceleration, heat transfer, and the capability to produce unsteady and steady-state solutions. Fluid properties are obtained from the reference fluid thermodynamic and transport properties (REFPROP) database [6] available from the National Institute for Standards and Testing (NIST). This database uses state-of-the-art equation-of-state models to fully describe fluid properties over a wide range of thermodynamic conditions, including liquid, vapor, mixed-phase and supercritical fluid regimes. Properties that completely define the fluid thermodynamic state, as well as transport properties, are available as a function of any two thermodynamic parameters. Validated fluid models for over 80 pure fluids and over 180 fluid mixtures are available in the database. The database is accessed through a suite of Fortran77 subroutines that are linked to the flow solver and are used to obtain fluid equation-of-state model parameters.

Fluid friction and heat transfer are modeled as source terms in the governing equations. This approach allows the flow to be modeled as one-dimensional and facilitates computational efficiency. Friction (i.e., viscous and minor losses) and heat transfer coefficients are obtained from suitable correlations between the flow variables and the source terms. The focus of this paper is to document the governing equations and numerical techniques used in the baseline solution of single-phase transient flow problems in the absence of heat transfer and potential energy.

III. Governing Equations

The governing equations consist of the quasi-one-dimensional continuity, Navier–Stokes, and energy equations simplified to model viscous effects and general acceleration in a noninertial frame using source terms:

$$\frac{1}{V}\frac{\partial UV}{\partial t}+\frac{\partial F}{\partial x}=\frac{S}{V} \tag{1}$$

$$U=\begin{vmatrix}\rho\\ \rho u\\ E\end{vmatrix},\qquad F=\begin{vmatrix}\rho u_r\\ (\rho u u_r+p)\\ \rho u_r H\end{vmatrix}$$

$$S=\begin{vmatrix}0\\ \frac{pV}{A}\frac{\mathrm{d}A}{\mathrm{d}x}-\rho V a_r-\tau_w\,\mathrm{d}x A_p-K\frac{\rho u_r^2}{2}A\\ \frac{\dot{q}}{V}\end{vmatrix} \tag{2}$$

where ρ is the density, u is the absolute velocity in the inertial frame, u_r is the relative velocity in the noninertial frame, a_r is the gravitational and relative acceleration in the noninertial frame, E is the total energy, p is the pressure, H is the stagnation enthalpy, V is the local cell volume, A is the local line cross-sectional area, dx is the cell line length, A_p is the perimeter, τ_w is the wall shear stress, and K is the local minor loss coefficient. The wall shear stress can be written in terms of a friction factor f, which is a function of the local Reynolds number and the wall surface roughness. For the viscous-flow examples presented later, the Churchill correlation [7] was used to determine single-phase friction factors using the following equation:

$$f=\frac{\tau_w}{\rho u_r^2}=\left[\left(\frac{8}{Re}\right)^{12}+\frac{1}{(A+B)^{3/2}}\right]^{1/12}$$
$$A=\left[2.457\,\ell n\left(\frac{1}{(7/Re)^{0.9}+0.27(\varepsilon/D)}\right)\right]^{16} \tag{3}$$
$$B=\left(\frac{37,530}{Re}\right)^{16}$$

where Re is the local Reynolds number based on hydraulic diameter. The minor loss coefficient K may be specified at various locations within the solution domain to model pressure loss at elbows, bends, valves, and sudden cross-sectional area changes.

Closure between the fluid pressure, density, and energy is performed with an equation of state for real fluids provided by the NIST REFPROP suite of thermodynamic routines. This allows for the solution of compressible, incompressible, and two-phase flows using the same computational procedure.

IV. Numerical Methods

Equations (1) and (2) may be solved with a variety of numerical schemes that are second-order accurate in space and time for steady or transient flow. The solution schemes implemented here include implicit, point-implicit, and explicit time-marching procedures, all of which will be described and demonstrated later. Multiple-grid-convergence acceleration may be used for steady-flow problems as well as during the inner iteration of time-accurate, point-implicit solutions to dramatically reduce the required number of computational iterations. Multiple numerical schemes were developed using the current procedure to provide flexibility and robustness when solving different flow conditions. These schemes allow for the fastest solution turnaround for the desired resolution of unsteady-flow physics. All of these numerical schemes use a node-centered, second-order spatially accurate, central-differenced discretization. The primary variables contained in the U vector of Eq. (2) are located at the nodes, which are typically spaced equally between the inlet and exit of each line in the overall domain.

A. Implicit Simulink Method

The Simulink version of the flow solver is implemented using an S-function programmed in ANSI C. This is the first time that Simulink has been demonstrated for the detailed transient flow solution in a quasi-one-dimensional real-fluid network. An S-function is a specialized program for use in Simulink models that contains specific subroutines required during model execution. The most important of these subroutines defines the time derivatives of the flow states $\mathrm{d}U/\mathrm{d}t$ at each computational node. So for N nodes, this subroutine must define three N derivatives, one for each element of the state vector U at each node. The state fluxes at each cell center are computed, as discussed later (Sec. IV.B), and the fluxes are distributed to the neighboring nodes. Once the time derivatives of the system states are computed, standard Simulink solvers are used to integrate the derivatives and compute the time history of the model states. Equations (1) and (2) may be solved iteratively in a sequential manner. One Simulink solver used here, `ode15s`, treats the discretized form of Eqs. (1) and (2) as a sequential set of ordinary differential equations and solves them iteratively with a Newton

iteration according to the numerical differentiation formula [8]:

$$\sum_{m=1}^{k} \frac{1}{m} \nabla^m U_{n+1} - \Delta t \left[-\frac{\partial F}{\partial x} + S \right] = 0 \tag{4}$$

where k is the temporal order of accuracy of the scheme. In the current investigation, both the temporal and spatial accuracy are second order. Another Simulink solver used here, `ode23s`, is a linearly implicit formula for stiff systems based on a modified Rosenbrock method that is especially effective with crude tolerances [8]. Both of the Simulink solvers covered here are discussed in detail in [8].

B. Explicit Method

Explicit time marching of Eqs. (1) and (2) may also be performed using a Lax–Wendroff control-volume scheme, as described by Ni [9]. This is the first implementation of the Lax–Wendroff/Ni scheme for transient real fluids. In this procedure, time-marching the primary variables U corresponds to an update in time at each node according to a second order temporally accurate Taylor series formula:

$$U_i^{n+1} = U_i^n + \frac{\partial U}{\partial t}\Delta t + \frac{\partial^2 U}{\partial t^2}\frac{\Delta t^2}{2} = U_i^n + \partial U_i + \partial^2 U_i \tag{5}$$

The Ni [9] scheme is a finite volume integration method. The scheme is applied in a three-step process. First, the *change* $\Delta t\ \partial U/\partial t$ [the second term on the right-hand side of Eq. (5)] at the center of each computational cell is approximated as

$$\Delta U = \frac{\Delta t}{\Delta x}(F_i^n - F_{i+1}^n) \tag{6}$$

The time-step size is determined by the Courant–Friedrichs–Lewy condition; that is,

$$\Delta t \le \frac{\mathrm{CFL}\Delta x}{|u_r + c|} \tag{7}$$

where CFL is the stability number with a typical value of 0.7 and c is the local speed of sound.

The *correction* $0.5\ \Delta t^2\ \partial^2 U/\partial t^2$ [the third term on the right-hand side of Eq. (5)] to the points i and $i+1$ are determined from time derivatives of Eq. (6). These corrections are then added or subtracted to the cell center *change* given by Eq. (6) to obtain the time-rate contributions to the adjacent nodes from each cell:

$$(\partial U_i + \partial^2 U_i)_{\mathrm{cell}} = \frac{1}{2}\left[\Delta U - \frac{\Delta t}{\Delta x}\Delta F\right] \tag{8}$$

$$(\partial U_{i+1} + \partial^2 U_{i+1})_{\mathrm{cell}} = \frac{1}{2}\left[\Delta U + \frac{\Delta t}{\Delta x}\Delta F\right] \tag{9}$$

where

$$\Delta F = \left(\frac{\partial F}{\partial U}\right)\Delta U \tag{10}$$

The primary variables at the nodes are then updated by

$$\delta U_i = (\partial U_i + \partial^2 U_i)_{\mathrm{cell}_i} + (\partial U_{i+1} + \partial^2 U_{i+1})_{\mathrm{cell}_{i-1}} \tag{11}$$

$$U_i^{n+1} = U_i^n + \delta U_i \tag{12}$$

The CFL stability number that determines the time-step size is set to 0.7, due to the explicit nature of this scheme. For steady flows or the inner iteration of the point-implicit technique described later, a multiple-grid acceleration procedure described by Ni [9] is used to greatly reduce the number of time steps to reach convergence. This allows the computational efficiency of this scheme to be competitive with the implicit procedure already described.

C. Point-Implicit Method

A point-implicit procedure can be made up from either the implicit or explicit schemes already described. For this procedure, the time-rate changes in Eqs. (4) and (5) are assumed to be in pseudotime. A true time derivative of the primary variables is added to the right-hand side of Eq. (1). This true time derivative is derived from stored solutions of the primary variables at $k+1$ previous time steps, where k is the temporal order of accuracy desired. An inner iteration is then used to drive the right-hand side to zero. The advantage of this approach is that steady-flow acceleration techniques may be used during the inner iteration, such as a multiple-grid scheme. Also, this technique provides flexibility in performing multiple lines of a network in parallel. This procedure is known as the dual-time-step technique [10] and has many similarities to the Newton iteration used in the implicit procedure.

D. Boundary Conditions

Boundary conditions are applied at each time step at the inlet and exit of each line in the network. These boundary conditions are specified based on the network connectivity and consist of either a global inlet, global exit, or junction boundary condition. At the global inlet(s) to the network, the stagnation enthalpy and entropy are held constant at levels determined from specified stagnation pressure and stagnation temperature and the predicted velocity. The resulting density and internal energy are determined from REFPROP, thus allowing for the determination of the total energy E. At the global exit (s) to the network, the specified exit static pressure is held constant. The internal energy and predicted velocity, along with this specified pressure, are used with REFPROP to determine the density and total energy. The prescribed inlet stagnation pressure, stagnation temperature, and exit static pressure may be specified as functions of time. At line junctions, the contributions of the time-rate changes in the primary variables contained in U of Eq. (1) are summed to give the total time-rate change at the junction node. For each junction of a given line, the neighboring line numbers and boundaries (i.e., inlet or exit) are stored to make the implementation of this boundary condition straightforward.

V. Results

Transient pipe flow simulations of gaseous nitrogen and liquid water were performed to verify the accuracy and demonstrate the capability of the present procedure. A coplanar ($z = 0$) two-pipe system, shown in Fig. 1, consisting of two 0.127-m (5-in.) pipes with 0.0254-m (1-in.) diameters was used for these simulations. The surface roughness of the pipe, necessary for viscous-flow simulations, was 2.54×10^{-6} m (0.0001 in.). The inlet stagnation

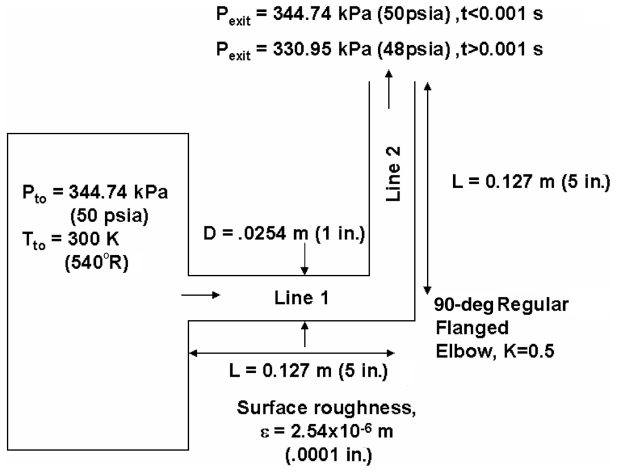

Fig. 1 Two-pipe system.

pressure, as well as the initial exit static pressure, was held at 345 kPa (50 psia). Thus, the initial velocity of the flow in the pipe was zero. The inlet stagnation temperature was held at 300 K (540°R). At time 0.001 s, the exit pressure was reduced to 331 kPa (48 psia). This sudden reduction in pressure initiates a series of expansion and compression waves through the pipe system and an increase in the velocity of the flow. For inviscid-flow cases, the pressure decays in the pipe to a uniform value and the velocity grows asymptotically to a uniform value. For viscous-flow cases, the pressure in the pipe decays, but to a nonuniform distribution, with the inlet pressure higher than the exit, due to friction and minor losses. The velocity of the pipe flow, however, once again grows asymptotically in time until it reaches a near-uniform value. The velocity in these cases was purposely kept low so that verification of the equilibrium (steady) solution could be made with incompressible pipe flow theory. All simulations were run in time until both the pressure and velocity distributions through the pipe remained time-independent. A grid-convergence study was performed in which 9, 17, 33, 65, and 129 uniformly spaced grid points were used along each pipe. The unsteady simulations with grid densities greater than or equal to 33 points per pipe predicted essentially the same waveforms, frequencies, and amplitudes, indicating that grid-convergence occurred with 33 points over each 0.127-m (5-in.) pipe. The converged *steady-state* pressure losses and velocities were also predicted to be the same, with grid densities greater than 33 points per pipe. The simulation results with 33 grid points are shown later.

A. Transient, Viscous, Nitrogen Pipe-System Flow

The two-pipe flow simulation with nitrogen is meant to test the current procedure's capabilities for modeling gaseous flow. Although the current test case corresponds to low-speed flow, additional test cases were executed with lower exit pressure and greater velocities, such that greater compressibility effects were present. Similar flow physics and agreement between the Matlab/Simulink and Fortran95 codes was obtained for those cases, as shown later. The explicit and point-implicit numerical procedures were run to verify the solution accuracy and to demonstrate features of these solution techniques. Figure 2 shows the predicted pressure and velocity as functions of time, using the explicit numerical technique for viscous flow at five locations along each pipe. In this scheme, the time-step size is determined by the minimum time step of all cells in the overall domain. The sinusoidal variation of pressure with time is evidence of the expansion and compression waves propagating through the pipe. The time variation of the velocity corresponds to these waves. The pressure decays in time until it reaches equilibrium, with an overall pressure drop across the system of 5.47 kPa (0.793 psia). The maximum pressure drop occurs at the exit of line 1 and the inlet of line 2, in which minor losses occur due to the flow turning in the 90-deg elbow. The velocity increases until it reaches a value of 65.59 m/s (215.2 ft/s). The friction factor predicted by Eq. (3) was 0.00188. The Reynolds number of the flow based on line diameter was predicted to be 3.66×10^5. Similar results were obtained using the time-accurate implicit Simulink solvers `ode15s` and `ode23s`.

The solution upon reaching steady state may be compared with an analytical solution to the energy equation. For incompressible flow, the control-volume energy equation may be written as

$$-h_{\text{friction}} = \left(\frac{p}{\rho g} + \frac{u_r^2}{2g} + z\right)_{\text{out}} - \left(\frac{p}{\rho g} + \frac{u_r^2}{2g} + z\right)_{\text{in}} \tag{13}$$

where h_{friction} is the viscous friction head, g is the acceleration due to gravity, and z is the potential height above a reference location. At the inlet to the configuration, shown in Fig. 1, the pressure is equal to the stagnation pressure and the velocity is zero. At the exit to line 2, the pressure is equal to the exit static pressure. The friction head may be written in terms of the friction and minor loss coefficients as

$$h_{\text{friction}} = \left(8f\frac{L}{D_h} + \sum_{\text{minor losses}} K\right)\frac{\rho u_r^2}{2} \tag{14}$$

where L is the pipe length, and D_h is the hydraulic diameter. For the problem described in Fig. 1 using nitrogen as the fluid, the analytical

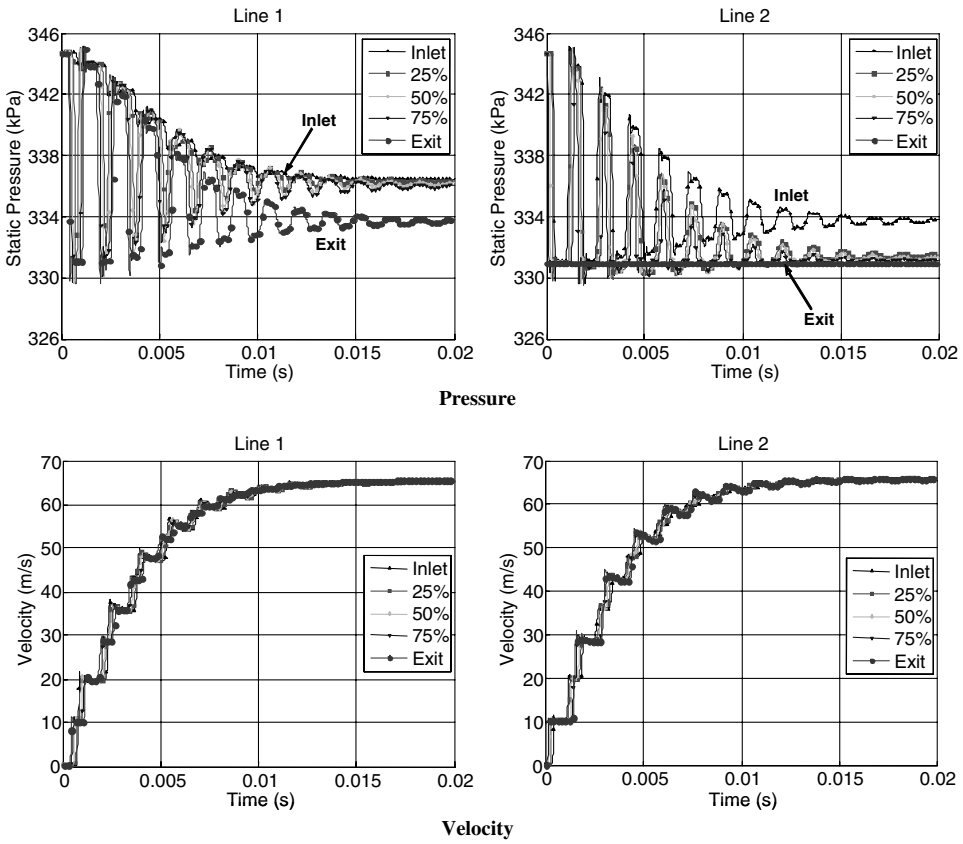

Fig. 2 Nitrogen transient viscous pipe flow using explicit numerical technique.

Table 1 Comparison between predicted and analytical results

Case	Num tech	Predicted ΔP, kPa	Analytic ΔP, kPa	% dif	Predicted velocity, m/s	Analytic velocity, m/s	% dif	Predicted freq, Hz	Analytic freq, Hz	% dif
Nitrogen	Explicit	5.47	5.45	0.37	65.59	65.67	0.12	637	696	8.5
	Point-implicit	5.47	5.45	0.37	65.11	65.67	0.85	N/A	N/A	N/A
Water	Point-implicit	5.59	5.61	0.36	4.05	4.05	0.0	2933	2959	0.88
	Simulink-implicit	5.58	5.61	0.53	4.06	4.05	0.2	2933	2959	0.88

solution of Eq. (13) results in a steady-state velocity of 65.67 m/s (215.4 ft/s) and a pressure drop of 5.45 kPa (0.791 psia). The predicted velocity corresponds to a low enough Mach number (0.15) that the nitrogen gas can be assumed essentially incompressible. The agreement between the numerical prediction and the steady-state analytical solution is excellent, as shown in Table 1, with the minor differences being due to the low level of compressibility in the gas. The numerical solution shown in Fig. 2 took 5850 iterations to reach steady state over 0.0397 s in real time.

As a check of the transient response of the computational solution, the period of pressure oscillations can be compared with the period expected for frictionless flow (e.g., organ-pipe modes). The pressure waves inside the pipe will travel at slightly less than the speed of sound, and the difference is a result of friction losses. Thus, the pressure oscillations should occur close to the natural frequency of the pipe ($c/2L$), or 696 Hz. The observed oscillation frequency in the simulation is 637 Hz, which is lower than the natural frequency of the pipe. This corresponds to an 8.5% difference (see Table 1) and is believed to be due to the slight compressibility of the nitrogen in the computational solution. As will be shown later for water, for which the fluid in the computational solution is truly incompressible, this difference drops to 0.88%. Thus, it is felt that the method produces transient results, in keeping with physical expectations.

Figure 3 shows the predicted results for the same two-pipe system, with nitrogen using the point-implicit numerical procedure. In this procedure, the time-step size can be prescribed by the user to be any value that results in a desired solution time and resolution of temporal features in the flow. For the present case, the time-step size was set at 0.01 s, which was approximately 1700 times larger than that required for the explicit procedure. The capability to use a large time-step size in the point-implicit procedure allows for very fast solution time. However, as shown by comparing Figs. 2 and 3, resolution of the high-frequency waves and their effect on the pressure and velocity is lost as a result of the increased time-step size. The availability of different solution algorithms to the overall procedure allows for rapid solutions when fine temporal resolution is not needed and for detailed solutions when high temporal resolution of waves is required.

B. Transient, Viscous, Water Pipe-System Flow

A similar set of simulations was performed using the present procedure with water to demonstrate the capability to predict transient flows of incompressible fluids. The main critical difference with incompressible fluids is that the speed of sound and wave speeds are much larger than for compressible fluids. This makes the use of explicit numerical techniques quite time-consuming. Resolution of the detailed unsteady sinusoidal transients already shown with the explicit numerical technique is possible, but requires large compute times. The effects of the high-frequency waves are not always of interest, so that numerical techniques that can take large time steps and reduce solution time are often attractive.

Figure 4 shows the transient, point-implicit, viscous solution of water through the previously described configuration (Fig. 1). Note that the time to reach steady state for water is much longer than that

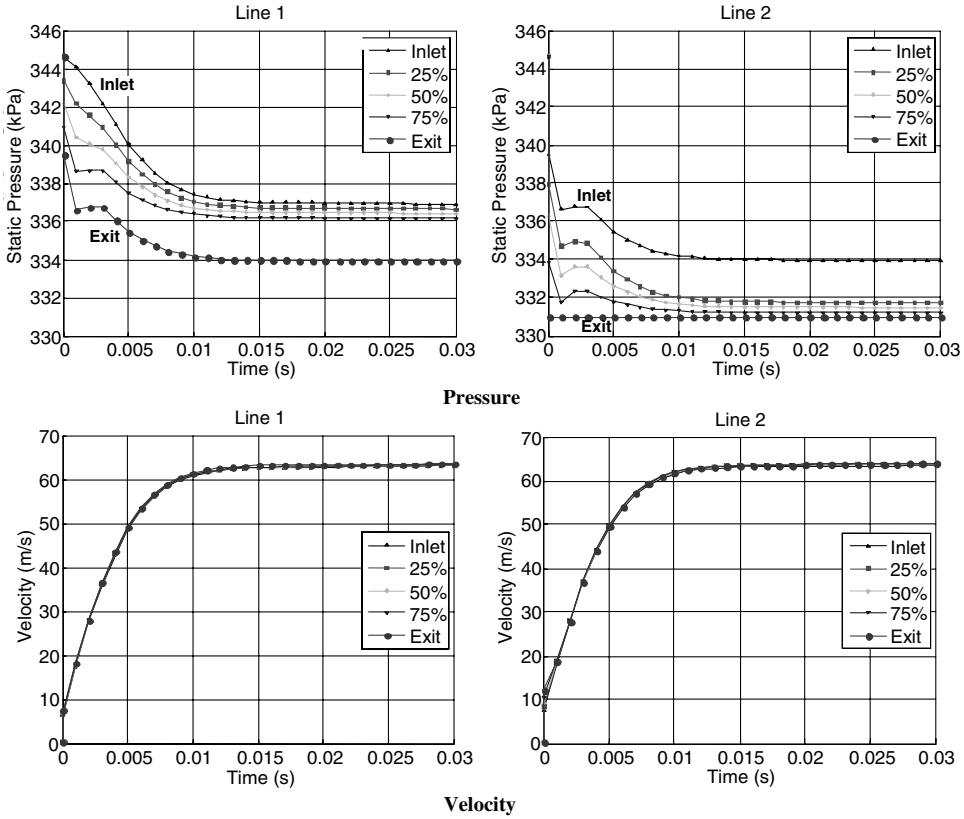

Fig. 3 Nitrogen transient viscous pipe flow using point-implicit numerical technique.

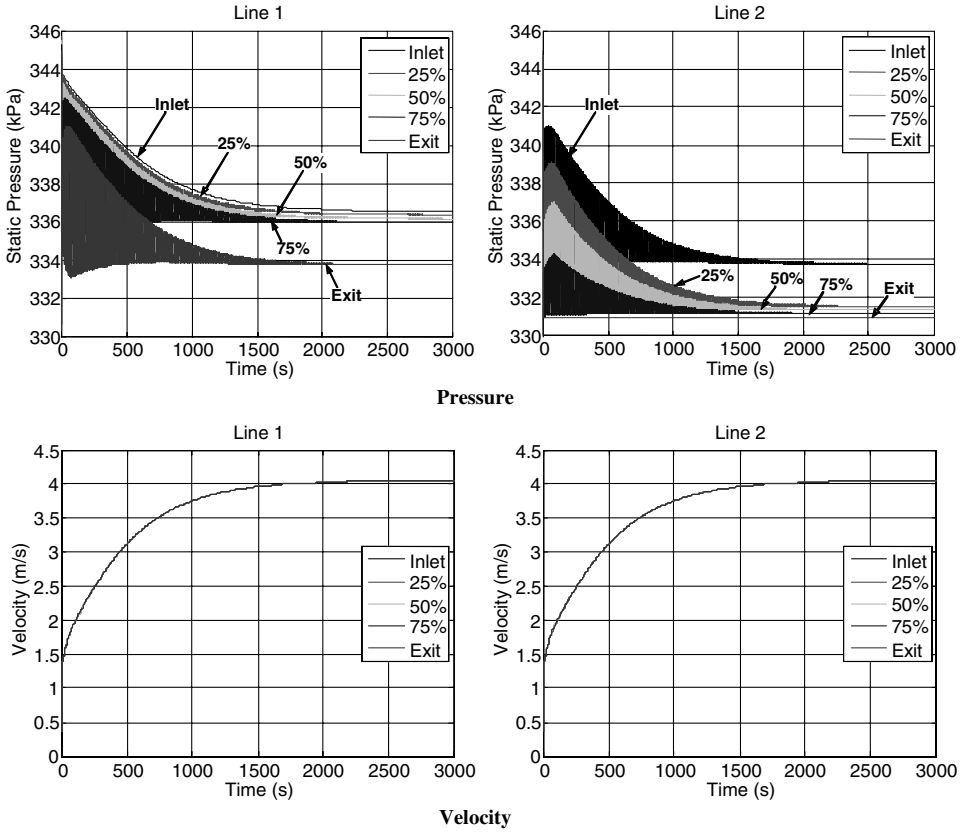

Fig. 4 Water transient viscous pipe flow using point-implicit numerical technique.

required for nitrogen, due to the incompressibility of the fluid. The size of the time step used in the point-implicit solution was 0.1 s. The time-step size required in the corresponding explicit solution procedure was approximately 2×10^{-6} s, or 50,000 times smaller than that used in the point-implicit solution. As a result, approximately 1.5 trillion time steps would be required to solve the 3000 s of time required to reach steady state. Even with a time-step size of 0.1 s, the point-implicit scheme still resolves much of the

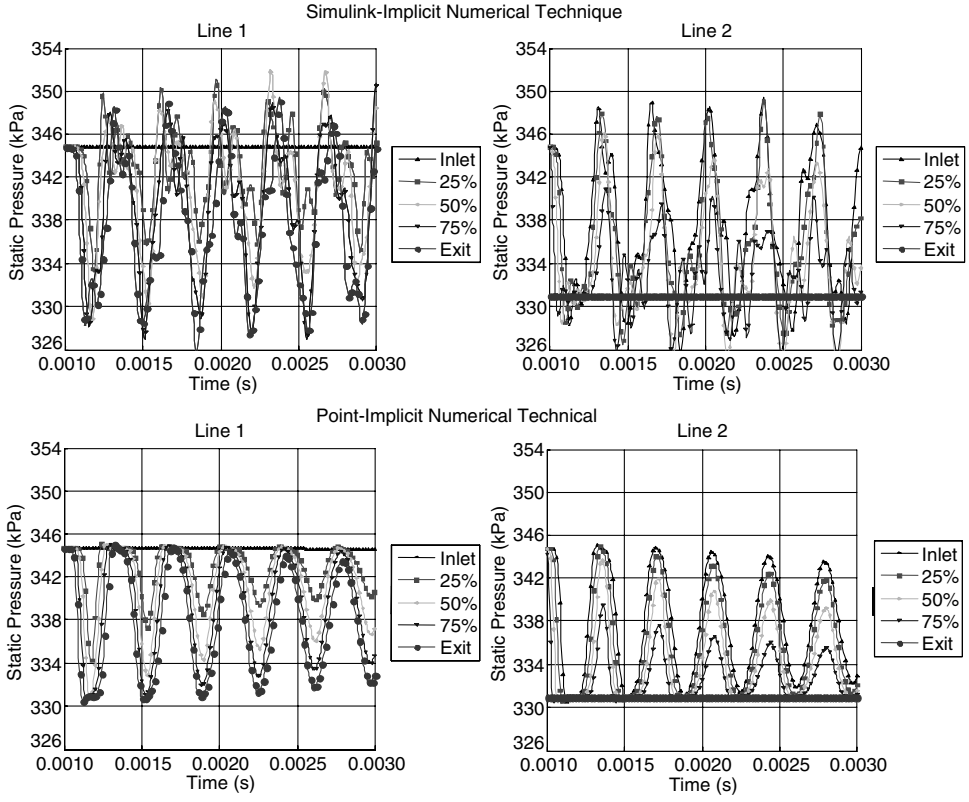

Fig. 5 Transient pressure comparison of numerical techniques for water transient viscous pipe flow.

pressure oscillations in the flow. The predicted pressure drop over the two-pipe system converges to a steady-state value of 5.59 kPa (0.811 psia), which is again in excellent agreement with the analytical energy equation analysis that gave 5.61 kPa (0.814 psia) (see Table 1). The velocity converges to a uniform steady-state value of 4.05 m/s (13.29 ft/s). The predicted friction factor was 0.00228 and the Reynolds number based on diameter was 1.06×10^5. The analytical energy equation analysis resulted in a velocity of 4.05 m/s (13.28 ft/s), demonstrating that the numerical techniques are verified against analytical solutions.

Figure 5 shows the predicted transient pressure over the time period between 0.001 and 0.003 s for both lines resulting from the Simulink-implicit numerical technique. Also shown in this figure is the predicted transient pressure over the same time period predicted with the point-implicit numerical scheme. The time-step size determined automatically in the Simulink-implicit technique (i.e., 2×10^{-5} s) was approximately 10 times greater than that which would have been used in the explicit technique. The same time-step size of 2×10^{-5} s was used in the point-implicit scheme. As with the point-implicit procedure, the fully implicit technique has the advantage of being able to use very large time-step sizes. This capability affords fast turnaround of solutions, with the possibility of some loss in temporal resolution. However, both of the implicit and point-implicit schemes also allow for small time-step sizes similar in magnitude to those used by the explicit numerical technique to resolve the transient details and frequencies in the flows, if desired. This ability to use a wide range of time-step sizes allows for maximum flexibility in obtaining the desired solutions.

Comparison of the unsteady pressure between the implicit and point-implicit numerical techniques in Fig. 5 shows that the predicted frequency of the unsteady waves is essentially the same. The observed pressure oscillation frequency of 2933 Hz compares well with the expected frequency of 2959 Hz based on frictionless flow analysis (see Table 1). The predicted amplitudes of the unsteady waves of the Simulink-implicit procedure are greater than those predicted by the point-implicit scheme. In addition, the Simulink-implicit procedure predicts more harmonics in the unsteady solution than predicted by the point-implicit scheme. These differences are likely due to a small dispersion error resulting from the adaptive time step used in the Simulink-implicit procedure and from the very strong temporal gradients caused by the instantaneous change in exit pressure. Comparison of the Simulink and point-implicit solutions at times greater than 0.003 s show diminishing differences in the transients of all variables.

VI. Conclusions

A new baseline procedure was developed for the numerical solution of transient quasi-one-dimensional flow (i.e., one-dimensional flow with area change) in system lines, networks, and volumes. The unique new features and results described include 1) the first-time use of Matlab/Simulink for detailed transient real-fluid network flows; 2) the first-time application of the Lax–Wendroff/Ni numerical scheme for transient real-fluid flows; 3) the implementation of multiple algorithms that enable the fastest solution turnaround for the desired resolution of unsteady-flow physics; 4) the documentation of two fundamental test cases of nitrogen and water, including unsteady pressure and velocity, that can be used by other researchers; and 5) back-to-back comparison of fundamental test cases between the Simulink and Fortan95 solvers and analytical theory.

Agreement between the numerical and analytical solutions based on energy-balance analysis and pressure oscillation frequency is excellent, demonstrating that the present procedure for the transient solution of compressible or incompressible fluids in the absence of heat transfer is valid. Unsteady pressure and velocity through the two lines in the system are shown as a demonstration of the transient physics predicted by the procedure.

Acknowledgments

The authors wish to acknowledge the U.S. Air Force Research Laboratory for funding this program under contract FA9300-04C-0008 and Sean Kenny, AFRL program manager for the Upper Stage Engine Technology (USET) program.

References

[1] Potter, M. C., and Somerton, C. W., *Thermodynamics for Engineers*, Schaum's Outline Series, McGraw–Hill, New York, 1993.

[2] Wallis, G., *One-Dimensional Two-Phase Flow*, McGraw–Hill, New York, 1969, Chap. 6.

[3] Wiley, E. B., *Fluid Transients in Systems*, Prentice–Hall, Upper Saddle River, NJ, 1997.

[4] Machmoum, A., and Seaïd, M., "A Highly Accurate Modified Method of Characteristics for Convection-Dominated Flow Problems," *Computational Methods in Applied Mathematics*, Vol. 3, No. 4, 2003, pp. 623–646.

[5] Mäkinen, J., Piché, R., and Ellman, A., "Fluid Transmission Line Modeling Using a Variational Method," *Journal of Dynamic Systems, Measurement, and Control*, Vol. 122, Mar. 2000, pp. 153–162.

[6] "NIST REFPROP, Reference Fluid Thermodynamic and Transport Properties," *NIST Standard Reference Database 23*, Ver. 7.0, National Inst. of Standards and Technology, Boulder, CO, 2002.

[7] Churchill, S. W., "Friction-Factor Equation Spans All Fluid-Flow Regimes," *Chemical Engineering*, Vol. 84, No. 24, Nov. 1977, pp. 91–92.

[8] Shampine, L. F., and Reichelt, M. W., "The Matlab ODE Suite," *SIAM Journal on Scientific Computing*, Vol. 18, No. 1, 1997, pp. 1–22.

[9] Ron-Ho, Ni., "A Multiple Grid Solver for Solving the Euler Equations," AIAA Paper 1981-1025R, 1981.

[10] Jameson, A., "Time Dependent Calculations Using Multigrid with Applications to Unsteady Flows Past Airfoils and Wings," AIAA Paper 91-1596, 1991.

C. Kaplan
Associate Editor